Asian Journal of Chemistry; Vol. 34, No. 10 (2022), 2639-2645

ASIAN JOURNAL OF CHEMISTRY

https://doi.org/10.14233/ajchem.2022.23900

Synthesis and Characterization of Nanocellulose from Lignocellulosic Agricultural Biomass by Acid Hydrolysis

J.K. PRASANNAKUMAR[1,*], G.K. PRAKASH[2], H.S. ONKARAPPA[3], B. SURESH[4] and B.E. BASAVARAJAPPA[1]

[1]Research Centre, Department of Chemistry, Bapuji Institute of Engineering and Technology (Affiliated to Visvesvaraya Technological University, Belagavi), Davangere-577006, India
[2]Department of Chemistry, Sri Taralubalu PU College, Davangere-577004, India
[3]Research Centre, Department of Chemistry, G.M. Institute of Technology (Affiliated to Visvesvaraya Technological University, Belagavi), Davangere-577006, India
[4]Department of Civil Engineering, Bapuji Institute of Engineering and Technology (Affiliated to Visvesvaraya Technological University, Belagavi), Davangere-577006, India

*Corresponding author: Fax: +91 8192 223261; Tel: +91 8192 222245; E-mail: prassvin@gmail.com

Received: 6 May 2022; *Accepted*: 29 June 2022; *Published online*: 19 September 2022; AJC-20967

The present study emphasizes lignocellulosic materials like agricultural biomass such as ragi stalk also known as Finger Millet Stalk *(Eleusine coracana)*, mango wood *(Mangifera caesia)* and groundnut husk (*Arachis hypogaea*) were transformed into cellulose by pretreatment with 5% NaOH and 5% $NaClO_2$ solution. In addition, the cellulose obtained was transformed into nanocellulose (NC) using acid hydrolysis, ultrasonication and centrifugation. The X-ray diffraction (XRD), scanning electron microscopy (SEM), Fourier transform infrared spectroscopy (FTIR) and thermogravimetry and differential thermal analysis (TGA/DTA) were used to characterize the synthesized nanocellulose. According to the FTIR findings, the chemical structure of cellulose synthesized from these agricultural biomasses was not affected by the synthetic approach, however, the synthetic procedure employed affects the morphology/surface topology of synthesized nanocellulose as confirmed by SEM. XRD studies reveal the crystalline and semi-crystalline nature of the synthesized nanocellulose. TEM monographs illustrate the surface structure and size of the synthesized nanocellulose ranging from 8 to 17 nm. The thermal stability of nanocellulose is revealed by TGA/DTA studies and the obtained nanocellulose shows thermal stability in the range of 240 to 327 ºC.

Keywords: Ragi stalk, Mango wood, Groundnut husk, Acid hydrolysis, Nanocellulose.

INTRODUCTION

Several studies have been performed in recent years to categorize materials that can be produced on a nanoscale while yet having the ability to lead civilization sustainably [1,2]. Cellulose is a biopolymer found naturally in plant cells such as wood and cotton and it is the most prevalent polymer in nature besides the primary ingredient of tree and plant cell walls. The highest cellulose content was found to be in cotton among all the plants and contains about 90% cellulose when compared to wood which contains up to 40-50% cellulose. The bast fibers, such as flax, hemp or ramie, comprise 70-80% cellulose. Aside from these, cellulose is found in various bacterial species, algae and sea tunicate [3]. Hence, it makes a considerable green nanotechnology material. Any crop containing lignocellulose, which comprises a set of plants, can be used as a precursor material for cellulose production. For nanocellulose synthesis, agricultural and wood wastes are used as raw materials. Source materials for nanocellulose extraction from parent cellulose have included olive tree biomass, cotton linter, cereal straws, banana plants and other materials [4].

Cellulose is a semi-crystalline polycarbohydrate consisting of anhydroglucose units (AGU) linked by chemical β-1,4-glycosidic bonds and consist of two repeating AGU having a "chair" conformation (Fig. 1). There are three hydroxyl functional groups in each of these units one primary and two secondary groups. Owing to the equatorial position of the hydroxyls, the AGU can form internal hydrogen bonds *i.e.* between the hydrogen atom of the C-3 hydroxyl group of one unit and the atom of the ring oxygen of the adjacent units [5,6].

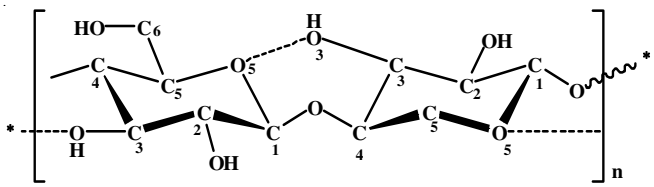

Fig. 1. Repeating unit of cellulose chain

Internal hydrogen bonds hinder glucopyranose rings from freely revolving around chemical glycoside bonds, increasing the stiffness of the cellulose chain [7]. Due to a strong intramolecular and intermolecular hydrogen bonds system of intramolecular and intermolecular hydrogen bonds, crystallites are orderly organized, stiff and strong cellulose components that are unattainable to water and some chemical reactions. Nanocrystalline amorphous regions with relatively weak hydrogen bonds, on the other hand, contribute to cellulose materials' greater hydrophilicity and accessibility. This biopolymer may establish hydrogen bonds due to the presence of (-OH) hydroxyl groups, making it a strong biopolymer [8]. Cellulose is a semicrystalline polymer that undergoes both amorphous and crystalline processes [9]. Nanocellulose is a new shape for this ancient and necessary natural polymer (NC). Over the years, Nanocellulose is an inimitable and natural compound extracted from native cellulose using different extraction methods. Nanocellulose is gaining popularity because of its unique surface shape and chemistry, superior physical and chemical strength and plenty of hydroxyl groups for modification. Furthermore, its substantial biological features, including biodegradability, biocompatibility and non-toxicity, as well as its environmental friendliness, make it stand out in nanoengineering and nanomanufacturing. It's been used in a variety of applications, including sensing devices [10,11]. Cellulose nanocrystals (CNCs) are natural materials that can be used in a variety of applications and are widely used in the paper and pharmaceutical industries. Various modifications of cellulose nanocrystals have been investigated. Nanocellulose is dispersible in multiple solvents due to a simple chemical modification of the cellulose surface. A strong acid approach is used to hydrolyze the cellulose obtained during the isolation process into nanocellulose [10]. Nanocellulose is used to make emulsions, biomedical devices, packaging and rheology modifiers like hydrogels used in the biomedicine, biocomposite films, supercapacitors and xerogels [11-17]. These applications demonstrate the potential of nanotechnology in the production of cellulose from lignocellulosic biomass.

Lignin, hemicellulose and cellulose are all known components of lignocellulosic biomass. Nanocellulose is made from cellulose, which is made from lignocellulosic material that has been pretreated and then the lignin was removed using an alkali treatment. The bleaching method removes hemicellulose [17]. The mechanical and chemical techniques can both be used to make nanocellulose from cellulose. The mechanical process involves the process of intensified ultrasonication or high-pressure homogenization and the chemical process involves acid hydrolysis (AH), ionic liquid (IL) and 2,2,6,6-tetramethylpiperidine-1-oxyl (TEMPO) [18-21]. When nanocellulose is hydrolyzed in acid, the amorphous zone is preferentially degraded, resulting in cellulose nanocrystals (CNC) with a rod-like shape and crystalline nature retained [22].

Natural nanocelluloses derived from HCl and H_2SO_4 are distinct. This method removes the amorphous region of cellulose, resulting in a structured cellulose nanocrystal (CNC) [23,24]. The NC obtained has high crystallinity and a diameter of less than 20 nm [25,26]. For example, nanocellulose synthesized using HCl is deficient in surface charge and subject to electrostatic repulsion. When nanocellulose is produced from H_2SO_4, a colloidal suspension is obtained [27]. When compared to the above-mentioned methods, acid hydrolysis of cellulose is more convenient in terms of time, cost and accessibility of acid. Thus, in current work, acid hydrolysis technique was used to synthesize nanocellulose from naturally occurring agricultural biowaste such as ragi stalk, mango wood and groundnut husk, alleviating the strain on the agricultural sector in India to use natural feedstock. Numerous studies have investigated the utilization of mechanical treatment methods such as sonication, high-speed blender, high-pressure homogenization, ultrafine grinder and ball mill to generate nanoscale fibers [28]. This procedure, however, is inefficient at separating hemicellulose, cellulose and lignin. Sonication and chemical treatment can be used in conjunction to produce pure CNC. There are a number of methods for producing pure cellulose fibers, but sonication has been found to be the easiest of them all. Pure CNCs can be produced by using sonication and chemical treatment. To create pure cellulose fibers, the sonication approach has been found to be the easiest mechanical treatment to use in conjunction with conventional chemical treatments [29,30].

Biomass derived from farming the raw materials employed in this work to isolate nanocellulose by acid hydrolysis are ragi stalk, mango wood and groundnut husk. The functionality, crystallinity, surface morphology and thermal stability of all synthesized nanocellulose were examined using FTIR, XRD, SEM, TEM and TGA/DTA. In this study, the sonication effect on the crystalline structure of the nanocellulose, which was not emphasized more in previous research. Hence, this method gives a new insight to establish the prospective applications of nanocellulose in the field of science and technology.

EXPERIMENTAL

Lignocellulosic materials like agriculture biomass were collected from farmlands in and around Davanagere, India. Sulphuric acid (H_2SO_4), sodium chlorite ($NaClO_2$), acetic acid (CH_3COOH) and sodium hydroxide (NaOH), were purchased from Qualigens and Merck chemicals. All compounds were utilized as such, with purity ranging from 98.0% to 99.0%.

Synthesis of cellulose: The procured lignocellulosic materials from agricultural biomass such as ragi stalk, mango wood and groundnut husk were separately and thoroughly washed and allowed to expose for sundry for one week then dried in a hot air oven, sieved into fine powder, the powder again dried in hot air oven till it gives constant weight. An appropriate measure of the individual sample was treated with 5% NaOH solution for 3-4 h by maintaining at 85-110 ºC with continuous stirring using a magnetic stirrer. The isolated cellulose residue

was filtered until it reached a neutral pH with distilled water. The obtained mass is washed with ether to make it moisture free, dried and stored for further process.

The bleaching was performed on the material obtained following alkali treatment by treating it with 5% $NaClO_2$ solution for 3-4 h by maintaining the acidic pH with glacial acetic acid at 85-110 ºC. By washing with distilled water, any remaining residual lignin was eliminated. After that, the filtration of cellulose was done repeatedly with deionized water before being brought to a neutral pH. Then this was oven-dried for one day or till it gives constant weight and processed for further preparations. Fig. 2 describes the detailed scheme of acid hydrolysis.

Synthesis of nanocellulose from acid hydrolysis: One of the most prominent ways of obtaining nanocellulose from cellulosic materials is acid hydrolysis. The acid may easily hydrolyze the disordered sections of cellulose chains, leaving the orderly parts intact.

To breakdown the glycoside bonds in cellulose, a strong acid such as H_2SO_4 or HCl is usually used. Acid hydrolysis is a multi-step process. Under monitored conditions such as concentration of acid, reaction time, temperature and acid to cellulose ratio. Addition of water to stop the acid hydrolysis process and upon subsequent centrifugation, dialysis to completely remove free acid molecules. Sonication forms a stable nanocellulose suspension followed by drying of the suspension yields solid nanocellulose [31-33]. This follows the mechanism shown in Fig. 3. To efficiently precede the hydrolysis reaction, water molecules and acid H^+ ions must infiltrate the cellulose fiber throughout this process. Otherwise, only the cellulose surface is affected by hydrolysis. Acid catalyzes the breakdown of long cellulose chains into shorter chain oligomers, which are then degraded by the acid. The hydrolysis of cellulose produces conjugated acid, which begins with an acidic proton and oxygen reaction that links two glucose units together. After the C–O bond is cleaved, the conjugate acid is broken down to the cyclic carbonium ion, which adopts a half-chair conformation. The rapid addition of water causes the release of free sugar and proton. The intermediate carbonium ion forms faster at the end of the polysaccharide chain than it does in the middle [34].

The conventional acid hydrolysis procedure was used to synthesize each sample. Cellulose sample (1 g) was added with 45 mL H_2SO_4 (55% w/v) and the aliquot mixture was kept for hydrolysis between 40-45 ºC for about 90 min with continuous stirring. Ice cold deionized water was poured to minimize hydrolysis. The resultant mass obtained was repeatedly washed with distilled water till it reaches neural pH followed by ultrasonication and centrifugation with 4000-5000 rpm for about 30-45 min to obtain AH-RSNC, AH-MWNC and AH-GHNC. They were kept in the refrigerator until needed. The yield of nanocellulose produced by this process was determined to be between 86% and 90%.

Characterization: Thermo Nicolet iS50 was used to record the FTIR of cellulose, AH-RSNC, AH-MWNC and AH-GHNC. The samples were pressed into thin pellets after being blended with KBr powder. The wavelength range of the sample was measured from 4000 to 400 cm^{-1}. The Bruker D8 advance diffractometer was used to record the XRD data. The peak heights of the crystalline and amorphous zones are measured

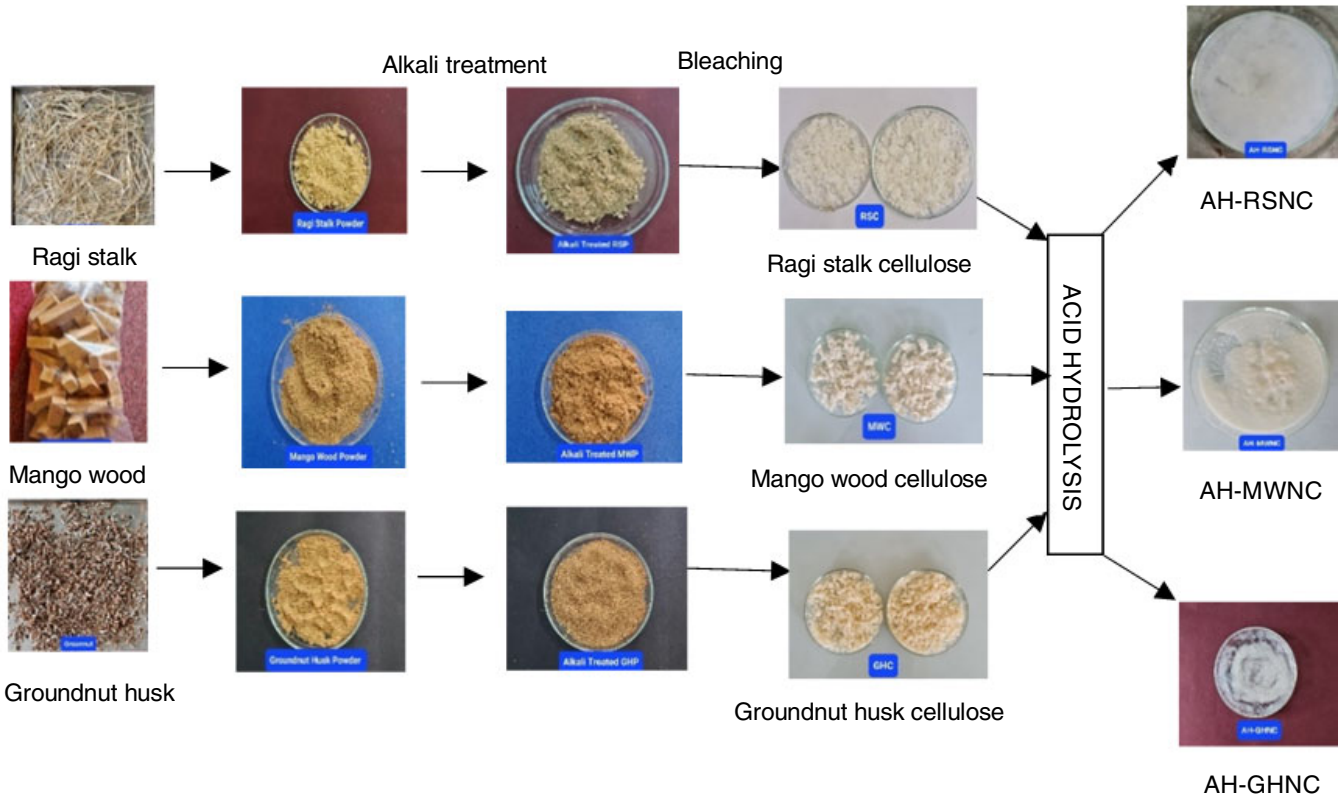

Fig. 2. Acid hydrolysis scheme

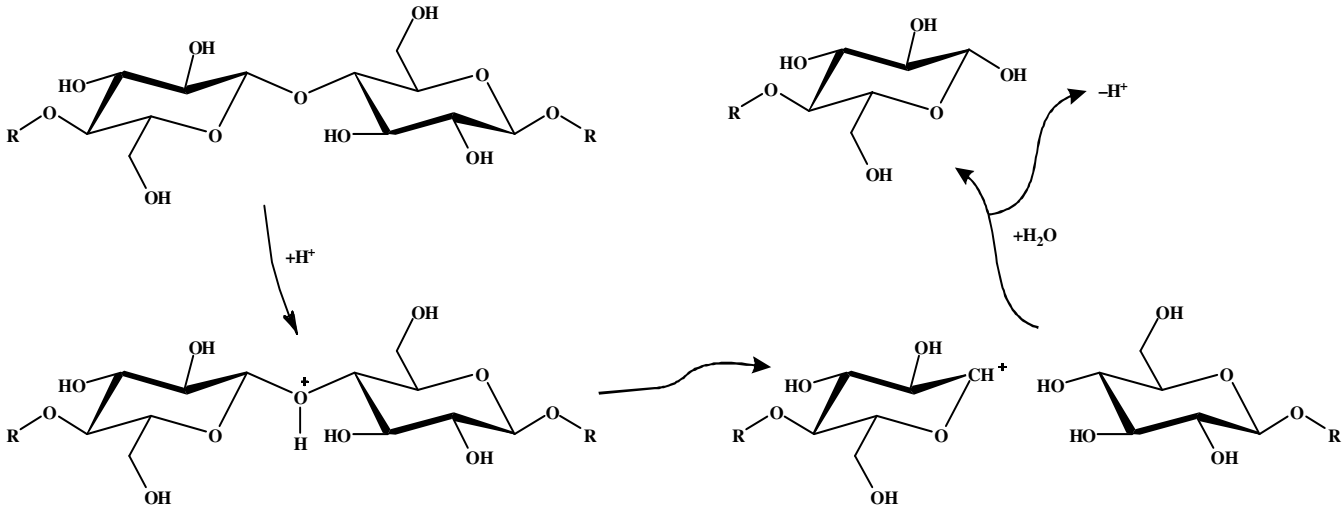

Fig. 3. Acid hydrolysis mechanism

and the crystallinity index (CI) was computed using Scherer's formula, with a step size of 0.02. The scanning electron microscopy (SEM) images were captured with the Jeol 6390LA/OXFORD XMX N instrument, which had an acceleration voltage range of 0.5 to 30 kV. The images were captured using a secondary electron (SE) detector. TEM images were recorded with 200 kV, LaB6 electron gun of point resolution 0.23 nm, lattice resolution 0.14 nm The Perkin-Elmer STA 6000 instrument was used for thermogravimetric and differential thermal analysis (TGA/DTA).

RESULTS AND DISCUSSION

In present study, the nanocellulose was extracted from the agricultural biomass using the acid hydrolysis method, which included pretreatment with alkali and bleaching. The synthe-sized nanocellulose's chemical group, crystallinity, surface morphology and thermal stability were evaluated using FTIR, XRD, SEM, TEM and TGA/DTA examinations.

FTIR studies: The chemical functionality of nanocellulose was examined using FTIR after various chemical treatments. The FTIR of cellulose, AH-RSNC, AH-MWNC and AH-GNC in Fig. 4. Peaks can be found in two main regions *i.e.* 3500 cm^{-1} to 2800 cm^{-1} in high wavenumbers and 1800 to 600 cm^{-1} in the lower wavenumbers.

The O-H stretching vibrations of the hydrogen-bonded hydroxyl groups in the cellulose molecules are shown by the broad absorption peaks at 3334.61 cm^{-1} to 3331.67 cm^{-1}. The C-H and CH_2 groups of cellulose stretching vibrations were attributed to the peaks at 2893.39 cm^{-1} and 2905.06 cm^{-1}, respectively. The H-O-H deformation vibration of the absorbed water and conjugated C=O stretch vibration are responsible for the peaks at 1644.34-1637.12 cm^{-1}. The C-H deformation was assigned to the small shoulder peaks vibrations at 1370.10 -1367.83 cm^{-1} (asymmetric). The O-H association band in cellulose was attributed to the curves at 1160.40-1104.00 cm^{-1}. The stretching (C-O) and rocking (C-H) cellulose peaks, which corresponded to the stretching (C-O) and rocking (C-H), respectively appeared at 1112 cm^{-1}. The cellulose, AH-RSNC and

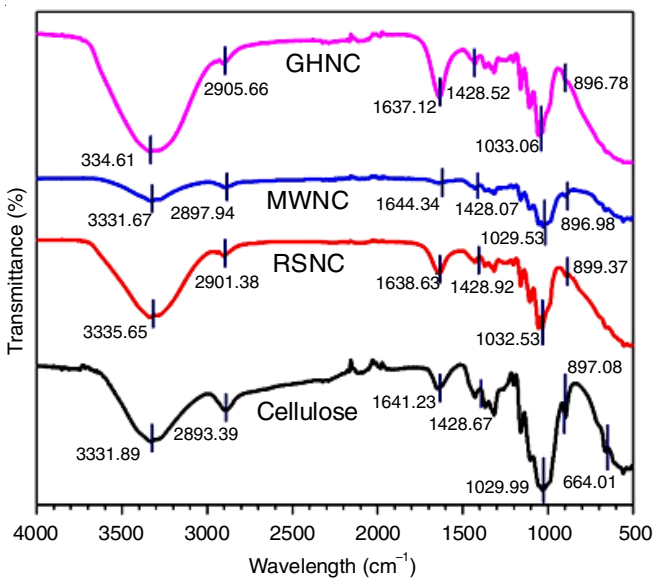

Fig. 4. FTIR of cellulose, AH-RSNC, AH-MWNC and AH-GNC

AH-MWNC peaks at 899.37-896.98 cm^{-1} correspond to the glycosidic linkage. The Out-of-plane bending causes a vibrational band at 664.01-557.88 cm^{-1}, which accounts for the aromatic C-H vibration in the cellulose range, implying that the removal of lignin is not favoured by chemical pretreatment. The aforementioned lignin vibrational peaks have decreased slightly in the AH-RSNC, AH-MWNC and AH-GHNC spectra, indicating that remaining lignin is eliminated during acid hydrolysis after cellulose is dissolved.

The chemical and ultrasonic treatments are required to separate lignin from strong hydrogen bonds in AH-RSNC, AH-MWNC and AH-GHNC. When water molecules absorb ultrasonic energy can cause more efficient cavitation, which includes the formation, expansion and disintegration of microscopic gas bubbles. The action of the ultrasound's hydrodynamic forces on the pulp causes the cellulose fibers to defibrillate. As a result, this method produces aggregated fibrils with a wide width distribution. Some cellulose fibers have been observed

to modify their crystalline structure after being subjected to ultrasonic treatment.

XRD studies: The X-ray diffraction (XRD) patterns were used to study the crystallinity, thermal and mechanical properties of three synthesized nanocelluloses. Cellulose, AH-RSNC, AH-MWNC and AH-GHNC XRD patterns are shown in Fig. 5, with 2θ values and peak intensities founded on the synthesis method. The crystallinity of the cellulose sample peaks at 2θ = 15.5º and 22.23º. The AH-RSNC exhibits crystallinity values of 2θ = 22.23º, 29.50º and 42.00º, while AH-MWNC exhibits crystallinity values of 2θ = 15.50º, 22.732º and 35.00º. The crystallinity values 2θ = 22.20º, 29.17º and 42.00º are shown in AH-GHNC, respectively. When compared to AH-RSNC and AH-GHNC, the cellulose and AH-MWNC show strong and intense peaks, indicating superior crystallinity. On the other hand, sonication does not affect the cellulose backbone's regular structure. However, AH-RSNC has a significantly wider peak at 29.50º and AH-GHNC has a little wider peak at 29.17º, Ultrasonic cavitation affects both crystalline and amorphous regions of cellulose, implying that the crystallinity index declines and that ultrasonic cavitation affect the crystalline and amorphous parts of cellulose simultaneously hinting that crystalline regions are destroyed. As a result, the crystallinity of AH-MWNC increased slightly, but ultrasonication had little effect on it. Only amorphous areas or crystalline defect regions are removed by this process. As the crystalline regions are more resistant to chemical treatments resulting in an increase in AH-MWNC crystallinity, which represents its hard and rigid nature. The fact that the crystallinity of AH-RSNC and AH-GHNC has decreased suggests that they are more flexible.

SEM studies: The synthesized nanocellulose is fibrous, semi-crystalline and fibrillar, according to the SEM monographs of AH-RSNC, AH-MWNC and AH-GHNC (Fig. 6). The average size of AH- RSNC is between 250 and 300 nm,

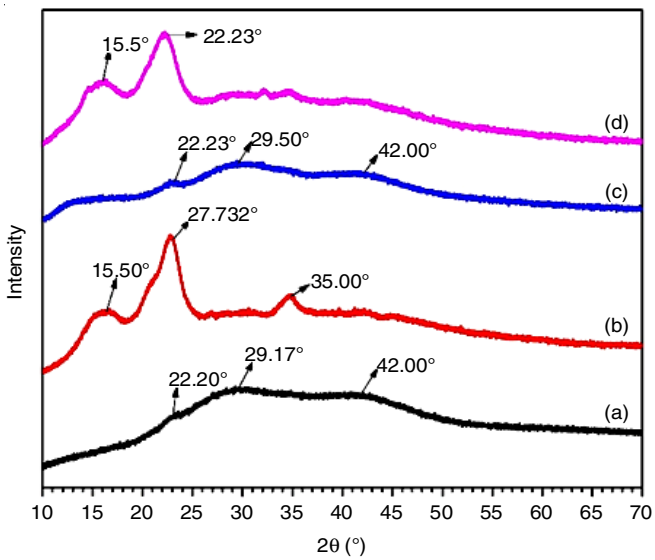

Fig. 5. XRD pattern of (a) AH-RSNC, (b) AH-MWNC, (c) AH-GHNC and (d) Cellulose

while AH-MWNC has an average size of 100-150 nm and AH-GHNC has a size of 250-300 nm. All the prepared nanocelluloses have lengths ranging from a few hundred nm to µm.

According to these findings, dimensions of the nanocellulose made from ragi stalk, mango wood and groundnut husk have different topologies in the nanoscale dimension. As a result, synthetic approaches have an impact on the size distribution and surface morphology and most of the disordered regions of cellulose were hydrolyzed during the acid hydrolysis process, leaving the fibrous-like nanocelluloses behind, resulting in a lower aspect ratio that is ideal for polymer reinforcement. The nanocellulose obtained has a fibrous and fibrillar shape, which facilitates the development of value-added products.

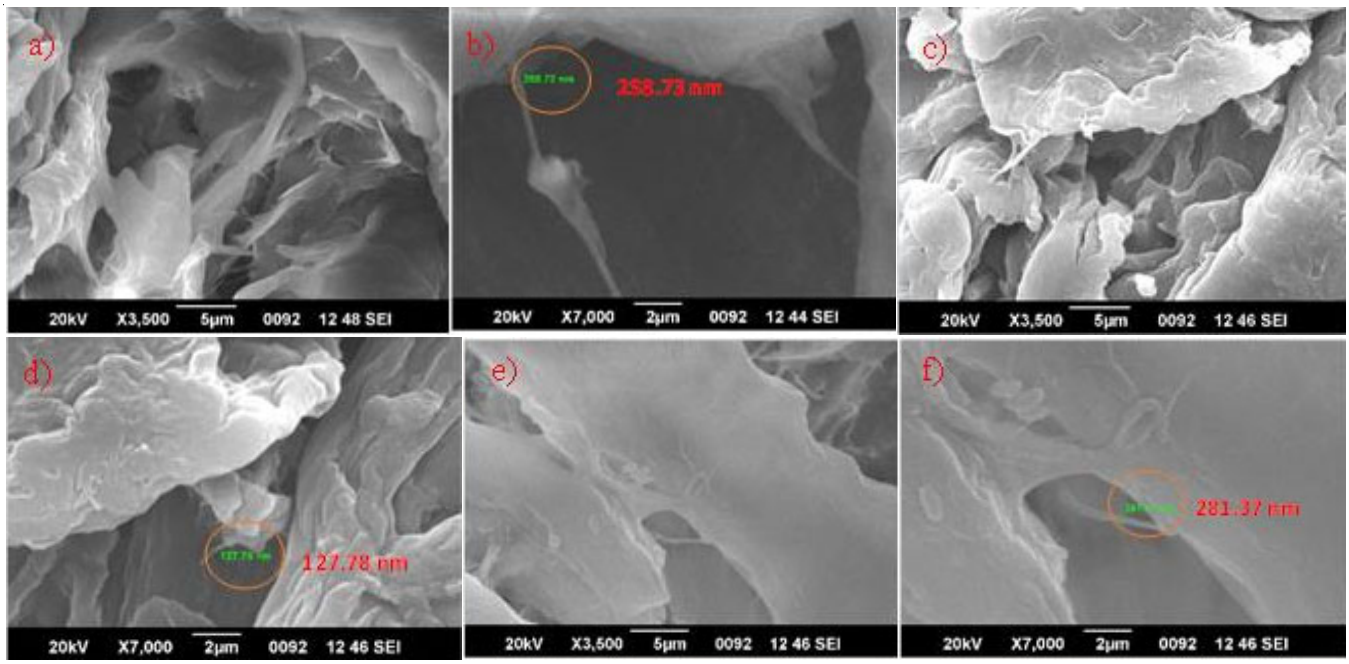

Fig. 6. SEM image of (a,b) AH-RSNC, (c,d) AH-MWNC and, (e,f) AH-GHNC

TEM studies: TEM morphologies were obtained for the analysis of the internal morphology and structure of the prepared sample. Fig. 7 clearly shows that the synthesized AH-RSNC, AH-MWNC and AH-GHNC samples have nanofibrils and nanofibrous structures. Nanofibers are well-separated and easily viewable. Across all the pictures, even the tendency to agglomerate can also be observed. This tendency can be attributed to the drying conditions during the preparation of samples that involved water evaporation. The AH-RSNC sample (7a-b) has a long elongated fibrous nature, with an average diameter of 9-14 nm. The AH-MWNC sample has non-fibrillar structures with an average size of 8-15 nm (Fig. 7c-d), whereas Fig. 7e-f shows that AH-GHNC sample contains nanofibrous structures with an average size of 8-17 nm.

Thermal studies: The thermal stability of the AH-RSNC, AH-MWNC and AH-GHNC was examined by TGA and DTA thermograms (Fig. 8). The temperatures at which the three types of nanocellulose degrade are as follows: AH-RSNC is 81 ºC, AH-MWNC is 327.57 ºC and AH-GHNC is 127.48 ºC. This is shown in the DTA curve as small troughs. The AH-RSNC shows the major weight loss at 81 ºC and the A-MWNC exhibits degradation at 250-327.57 ºC whereas AH-GHNC

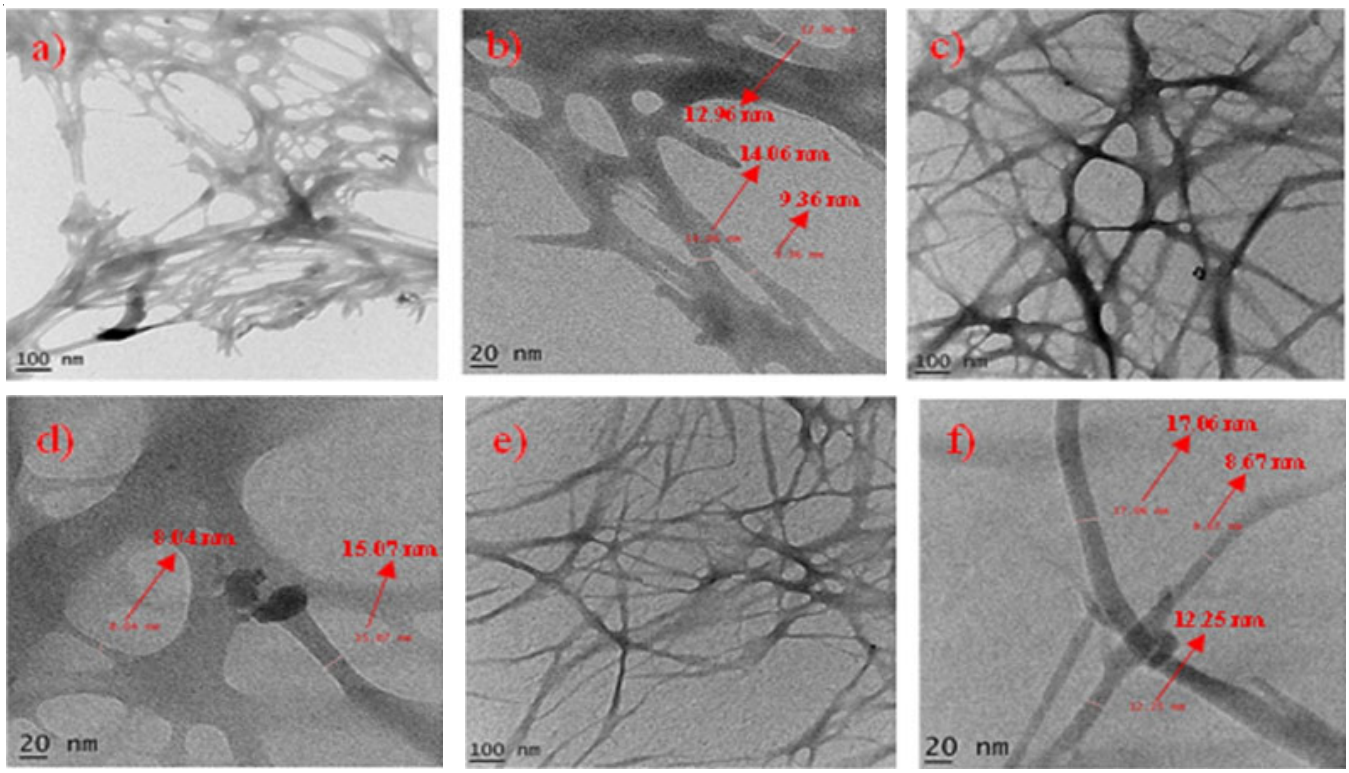

Fig. 7. TEM image of (a,b) AH-RSNC, (c,d) AH-MWNC and (e,f) AH-GHNC

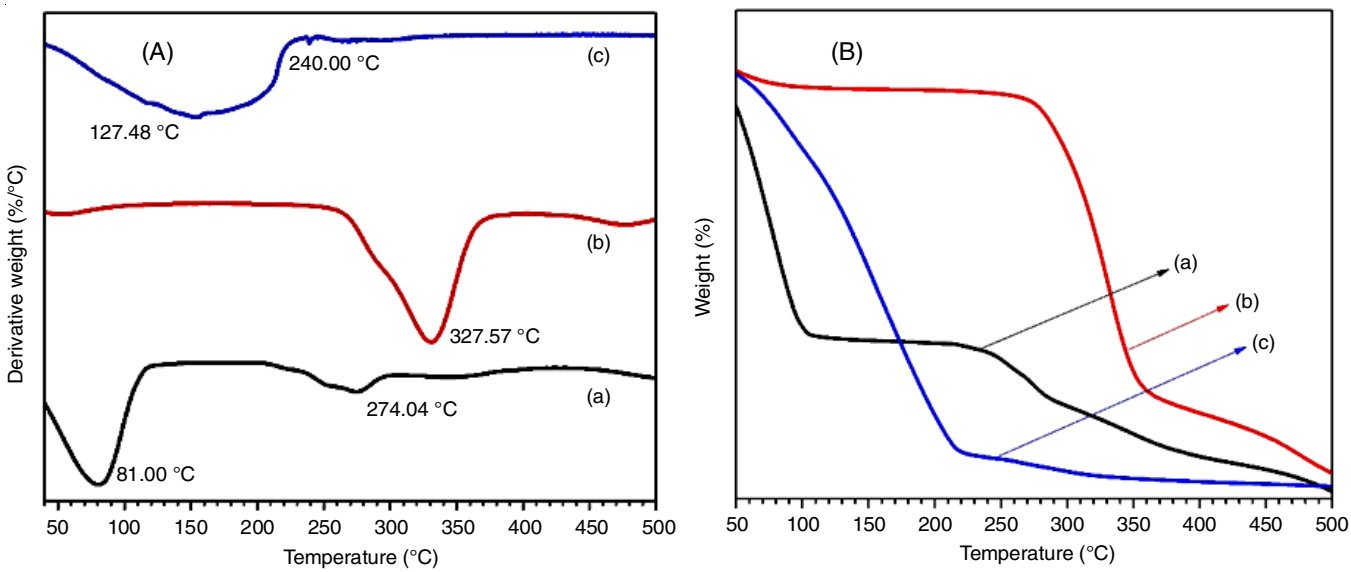

Fig. 8. (A) TGA and (B) DTG of (a) AH-RSNC, (b) AH-MWNC and (c) AH-GHNC

shows a weight loss at 100-127 ºC indicated that the nanocellulose degraded primarily as hemicellulose and the glycosidic linkages were broken and depolymerized. According to these studies, the AH-MWNC sample has the higher thermal stability as compared to other prepared samples.

Conclusion

In present work, different nanocellulose was extracted from the lignocellulosic materials like agricultural biomass ragi stalk, mango wood powder and groundnut husk by acid hydrolysis. The impact of synthetic methods on the nanocellulose characteristics and morphology was thoroughly examined. According to the FTIR comparison analysis, the synthetic techniques have no detectable effect on the primary functional group areas of cellulose. Acid hydrolysis demonstrates improved crystallinity. The SEM results showed that synthesized nanocellulose comes in a variety of nanoscale forms, including semi-crystalline, fibrous and fibrillar. The crystallinity and semi-crystalline nature of nanocellulose were depicted by XRD. The thermal analysis showed that the commencement of acid hydrolyzed cellulose degradation occured at 81 ºC, as indicated by the strong troughs in the DTA thermogram. The most important TGA finding is that acid hydrolyzed AH-MWNC (327.57 ºC) has a higher degradation temperature, indicating superior thermal stability. TEM monograph displays the nanometer-sized morphology and distribution of the synthesized ragi stalk, mango wood and groundnut husk. Furthermore, the purpose of this study is to demonstrate a viable application of synthesized cellulose from naturally accessible biomass, thereby addressing India's demand for solid waste management and minimizing chemical waste through a more realistic nanocellulose synthesis process.

CONFLICT OF INTEREST

The authors declare that there is no conflict of interests regarding the publication of this article.

REFERENCES

1. L. Pokrajac, A. Abbas, W. Chrzanowski, G.M. Dias, B.J. Eggleton, S. Maguire, E. Maine, T. Malloy, J. Nathwani, L. Nazar, A. Sips, J. Sone, A. van den Berg, P.S. Weiss and S. Mitra, *ACS Nano*, **15**, 18606 (2021); https://doi.org/10.1021/acsnano.1c10919
2. A. Yamaguchi, H. Sakamoto, T. Kitamura, M. Hashimoto and S.I. Suye, *Colloids Surf. B Biointerfaces*, **183**, 110392 (2019); https://doi.org/10.1016/j.colsurfb.2019.110392
3. M.J. Dunlop, C. Clemons, R. Reiner, R. Sabo, U.P. Agarwal, R. Bissessur, H. Sojoudiasli, P.J. Carreau and B. Acharya, *Sci. Rep.*, **10**, 19090 (2020); https://doi.org/10.1038/s41598-020-76144-9
4. E. Espinosa, R. Sánchez, R. Otero, J. Domínguez-Robles and A. Rodríguez, *Int. J. Biol. Macromol.*, **103**, 990 (2017); https://doi.org/10.1016/j.ijbiomac.2017.05.156
5. T. Hosoya, M. Bacher, A. Potthast, T. Elder and T. Rosenau, *Cellulose*, **25**, 3797 (2018); https://doi.org/10.1007/s10570-018-1835-y
6. R.J. Moon, A. Martini, J. Nairn, J. Simonsen and J. Youngblood, *Chem. Soc. Rev.*, **40**, 3941 (2011); https://doi.org/10.1039/c0cs00108b
7. M. Wohlert, T. Benselfelt, L. Wågberg, I. Furó, L.A. Berglund and J. Wohlert, *Cellulose*, **29**, 1 (2022); https://doi.org/10.1007/s10570-021-04325-4
8. A.C. Khazraji and S. Robert, *J. Nanomater.*, **2013**, 409676 (2013); https://doi.org/10.1155/2013/409676
9. M.L. Mansfield, *Macromolecules*, **20**, 1384 (1987); https://doi.org/10.1021/ma00172a036
10. H. Golmohammadi, E. Morales-Narváez, T. Naghdi and A. Merkoçi, *Chem. Mater.*, **29**, 5426 (2017); https://doi.org/10.1021/acs.chemmater.7b01170
11. O. Faruk, M. Sain, R. Farnood, Y. Pan and H. Xiao, *J. Polym. Environ.*, **22**, 279 (2014); https://doi.org/10.1007/s10924-013-0631-x
12. L.O. Pinto, J.S. Bernardes and C.A. Rezende, *Carbohydr. Polym.*, **218**, 145 (2019); https://doi.org/10.1016/j.carbpol.2019.04.070
13. E.S. Ferreira and C.A. Rezende, *ACS Sustain. Chem. & Eng.*, **6**, 14365 (2018); https://doi.org/10.1021/acssuschemeng.8b03071
14. J.P.S. Morais, M.F. Rosa, M.M. de Souza Filho, L.D. Nascimento, D.M. do Nascimento and A.R. Cassales, *Carbohydr. Polym.*, **91**, 229 (2013); https://doi.org/10.1016/j.carbpol.2012.08.010
15. Ú. Fillat, B. Wicklein, R. Martín-Sampedro, D. Ibarra, E. Ruiz-Hitzky, C. Valencia, A. Sarrión, E. Castro and M.E. Eugenio, *Carbohydr. Polym.*, **179**, 252 (2018); https://doi.org/10.1016/j.carbpol.2017.09.072
16. Y. Liu, Y. Sui, C. Liu, C. Liu, M. Wu, B. Li and Y. Li, *Carbohydr. Polym.*, **188**, 27 (2018); https://doi.org/10.1016/j.carbpol.2018.01.093
17. E. Espinosa, I. Bascón-Villegas, A. Rosal, F. Pérez-Rodríguez, G. Chinga-Carrasco and A. Rodríguez, *Int. J. Biol. Macromol.*, **141**, 197 (2019); https://doi.org/10.1016/j.ijbiomac.2019.08.262
18. P. Jagadesh, A. Ramachandramurthy and R. Murugesan, *Constr. Build. Mater.*, **176**, 608 (2018); https://doi.org/10.1016/j.conbuildmat.2018.05.037
19. N. Lin and A. Dufresne, *Eur. Polym. J.*, **59**, 302 (2014); https://doi.org/10.1016/j.eurpolymj.2014.07.025
20. S. Liu, G. Cheng, Y. Xiong, Y. Ding and X. Luo, *J. Hazard. Mater.*, **384**, 121195 (2020); https://doi.org/10.1016/j.jhazmat.2019.121195
21. L. Feng and Z.L. Chen, *J. Mol. Liq.*, **142**, 1 (2008); https://doi.org/10.1016/j.molliq.2008.06.007
22. W.T. Wulandari, A. Rochliadi and I.M. Arcana, *IOP Conf. Ser.: Mater. Sci. Eng.*, **107**, 012045 (2016); https://doi.org/10.1088/1757-899X/107/1/012045
23. M.S. Mohaiyiddin, H.L. Ong, M.B.H. Othman, N.M. Julkapli, A.R.C. Villagracia and H. Md. Akil, *Polym. Compos.*, **39**, E561 (2018); https://doi.org/10.1002/pc.24712
24. Y. Habibi, L.A. Lucia and O.J. Rojas, *Chem. Rev.*, **110**, 3479 (2010); https://doi.org/10.1021/cr90s0339w
25. B. Deepa, E. Abraham, B.M. Cherian, A. Bismarck, J.J. Blaker, L.A. Pothan, A.L. Leao, S.F. de Souza and M. Kottaisamy, *Bioresour. Technol.*, **102**, 1988 (2011); https://doi.org/10.1016/j.biortech.2010.09.030
26. F. Jiang and Y.L. Hsieh, *Carbohydr. Polym.*, **95**, 32 (2013); https://doi.org/10.1016/j.carbpol.2013.02.022
27. M.A. Hubbe, O.J. Rojas, L.A. Lucia and M. Sain, *BioResources*, **3**, 929 (2008); https://doi.org/10.15376/biores.3.3.929-980
28. M. Mahardika, H. Abral, A. Kasim, S. Arief and M. Asrofi, *Fibers*, **6**, 28 (2018); https://doi.org/10.3390/fib6020028
29. M. Asrofi, H. Abral, A. Kasim, A. Pratoto, M. Mahardika, J.W. Park and H.J. Kim, *Fibers Polym.*, **19**, 1618 (2018); https://doi.org/10.1007/s12221-018-7953-1
30. Y. Wang, X. Wei, J. Li, F. Wang, Q. Wang, Y. Zhang and L. Kong, *Ind. Crops Prod.*, **104**, 237 (2017); https://doi.org/10.1016/j.indcrop.2017.04.032
31. L. Brinchi, F. Cotana, E. Fortunati and J.M. Kenny, *Carbohydr. Polym.*, **94**, 154 (2013); https://doi.org/10.1016/j.carbpol.2013.01.033
32. N. Wang, E. Ding and R. Cheng, *Polymer*, **48**, 3486 (2007); https://doi.org/10.1016/j.polymer.2007.03.062
33. X.M. Dong, J.-F. Revol and D.G. Gray, *Cellulose*, **5**, 19 (1998); https://doi.org/10.1023/A:1009260511939
34. S. Sasmal and K. Mohanty, Pretreatment of Lignocellulosic Biomass toward Biofuel Production; In: Biorefining of Biomass to Biofuels, pp. 203-221, Springer, Cham (2018).